Experimental Eye Research 93 (2011) 771–777

Contents lists available at ScienceDirect

Experimental Eye Research

journal homepage: www.elsevier.com/locate/yexer

Letter to the editor

Specific deficits in visual electrophysiology in a mouse model of dominant optic atrophy

Alun R. Barnard [a,*], Peter Charbel Issa [a], Georgia Perganta [a], Pete A. Williams [b], Vanessa J. Davies [b,c], Sumathi Sekaran [a], Marcela Votruba [b,d], Robert E. MacLaren [a,e,**]

[a] Nuffield Laboratory of Ophthalmology & Oxford NIHR Biomedical Research Centre, University of Oxford, John Radcliffe Hospital, Oxford OX3 9DU, UK
[b] School of Optometry and Vision Sciences, Cardiff University, Cardiff CF24 4LU, UK
[c] Cardiff Neuroscience Centre, Cardiff University, Cardiff, UK
[d] Cardiff Eye Unit, University Hospital Wales, Cardiff CF14 4XW, UK
[e] Moorfields Eye Hospital NIHR Biomedical Research Centre, London EC1V 2PD, UK

ARTICLE INFO

Article history:
Received 17 May 2011
Accepted in revised form 16 July 2011
Available online 22 July 2011

Keywords:
optic atrophy
Opa1
retina
ganglion cell
ERG
VEP
electrophysiology

ABSTRACT

Autosomal dominant optic atrophy (ADOA) is a slowly progressive optic neuropathy caused by mutations in the *OPA1* gene. *OPA1* is ubiquitously expressed and plays a key role in mitochondrial fusion. Heterozygous *Opa1* mutant mice (B6; C3-*Opa1*^{Q285STOP}), have previously been reported to develop visual defects and optic nerve changes. In this study, *in vivo* visual electrophysiological testing (ERGs and VEPs) was performed on 11–13 month old B6; C3-*Opa1*^{Q285STOP} mice ($n = 5$) and age/sex matched wildtype littermate controls. Full intensity series were recorded in response to brief (4 ms) single flash stimuli delivered in a Ganzfeld dome under dark- and light-adapted conditions. The major ERG components (a-wave and b-wave) showed no detectable difference from wildtype in the amplitude or implicit time of dark-adapted ERGs across the full intensity range tested. This was also true for the components of the dark-adapted VEP. However, the light-adapted ERG responses revealed a significant reduction in the photopic negative response (PhNR) amplitude in *Opa1*$^{+/-}$ animals relative to wildtypes at the brighter intensities tested. Elements of the light-adapted VEP were also abnormal in mutant mice. Overall *Opa1*$^{+/-}$ mice display functional deficits in electrophysiology that are consistent with ganglion cell dysfunction. These deficits may correlate with a reduction in the dendritic arborisation of retinal ganglion cells, which has been previously reported to occur at a similar age in the same mutant mouse line (Williams et al., 2010). The functional phenotype we have described in this mouse model may be useful in the robust and accurate assessment of potential treatments for ADOA.

1. Introduction

Autosomal dominant optic atrophy (ADOA, OMIM 165500) is the most common inherited optic neuropathy, presenting with variable loss of visual acuity, central visual field defects, colour vision abnormalities and optic atrophy. It is associated with optic nerve degeneration and the ultimate loss of retinal ganglion cells (Votruba, 2004). Heterozygous mutations in *OPA1* cause ADOA (Alexander et al., 2000), likely through haploinsufficiency. The gene product of *OPA1* is ubiquitously expressed and plays a key role in mitochondrial fusion (Davies and Votruba, 2006). Despite this broad cell and tissue distribution, retinal ganglion cells appear to be specifically susceptible to mutations in *OPA1*, although there is increasing evidence that other cell types and neurological systems may also be affected (Amati-Bonneau et al., 2009; Yu-Wai-Man et al., 2010). The coding sequence of the *OPA1* gene is 2.9 kb in size, which, including regulatory sequences, is small enough to fit into recombinant adeno-associated virus (AAV) serotype 2; known to transduce primate ganglion cells highly effectively (Yin et al., 2011). Taken together with the slow degeneration and presumed haploinsufficiency mechanism in ADOA, this makes the disease appealing for future clinical trials using AAV2 mediated gene replacement.

Heterozygous *Opa1* mutant mice have been generated that carry a nonsense mutation in exon 8, which inserts a STOP signal instead of a glutamine amino acid (Q285X), and causes premature protein

* Corresponding author. Nuffield Laboratory of Ophthalmology, University of Oxford, Level 5 and 6 West Wing, The John Radcliffe Hospital, Headley Way, Oxford OX3 9DU, UK. Tel.: +44 (0) 1865 234 701; fax: +44 (0) 1865 234 795.
** Corresponding author. Nuffield Laboratory of Ophthalmology, University of Oxford, Level 5 and 6 West Wing, The John Radcliffe Hospital, Headley Way, Oxford OX3 9DU, UK. Tel.: +44 (0) 1865 234 782; fax: +44 (0) 1865 234 795.
E-mail addresses: alun.barnard@eye.ox.ac.uk (A.R. Barnard), enquiries@eye.ox.ac.uk (R.E. MacLaren).

0014-4835/$ – see front matter © 2011 Elsevier Ltd. All rights reserved.
doi:10.1016/j.exer.2011.07.004

truncation (Davies et al., 2007). Anatomical changes have been previously reported in this line, and include slow optic nerve degeneration, abnormalities in mitochondrial ultrastructure in ganglion cell axons and a progressive ganglion cell dendropathy (Davies et al., 2007; White et al., 2009; Williams et al., 2010). Identifying functional changes in the retina of *Opa1* mutant mice has been significantly more challenging. There is evidence of a reduction in visual acuity in *Opa1* mutant mice, as tested by responses to an optokinetic drum stimulus (Davies et al., 2007). However, the detection of a phenotype using a more direct measure of retinal function, such as the electroretinogram (ERG), would aid considerably in the preclinical assessment of potential treatments such as AAV.*OPA1* gene replacement. This would be particularly true if the functional deficit appeared at relatively early stages. A recent assessment in a different mouse model of *OPA1*-associated ADOA revealed a subtle reduction in amplitude (but not latency) in the cortical visually evoked potential (VEP) at 20 months, but no changes in retinal function were seen (Heiduschka et al., 2010).

Therefore, the purpose of our study was to re-examine and extend visual electrophysiological investigation in *Opa1* mutant mice. Particular emphasis was placed on recording and analysing specific components of the ERG that have been linked to the activity of retinal ganglion cells, such as the scotopic threshold response (STR) and the photopic negative response (PhNR). In our ADOA mouse model, a recent morphological study has shown that retraction of retinal ganglion cell dendrites is apparent from around one year, which is before the onset of ganglion cell and optic nerve degenerative changes (Williams et al., 2010). With this in mind, we investigated mice at a similar age to explore whether a deficit in the ganglion cell associated ERG components might be correlated with these morphological changes and reveal evidence of RGC dysfunction.

2. Methods

2.1. Animals and experimental preparation

Experiments were conducted on five 11–13 month old heterozygous B6; C3-*Opa1*^{Q285STOP} mice (*Opa1*$^{+/-}$, $n = 5$) and an equal number of age/sex matched wildtype littermate controls (*Opa1*$^{+/+}$, $n = 5$). All animal breeding and experimental procedures were performed under approval of local and national ethical and legal authorities. Generation and propagation of the mutant line has been described previously (Davies et al., 2007). Mice were kept in a 12 h light (<100 lux)/12 h dark cycle with food and water available *ad libitum*. All recordings were conducted 5–9 h after the light onset (dawn). Prior to testing all animals were dark-adapted for >90 min. Animal preparation and electrode placement were conducted under dim red illumination. Mice were anaesthetized with a single intraperitoneal injection of Dormitor (medetomidine hydrochloride, 1 mg/kg body weight) and ketamine (60 mg/kg body weight) in water. Pupils were fully dilated (to around 2 mm^2 in both groups) using 1% tropicamide eye drops.

2.2. In vivo electrophysiology

Electroretinogram (ERG) and flash visual evoked potential (VEP) responses were recorded simultaneously from electrodes placed on the cornea and overlying the visual cortex, respectively. For ERG recordings a DTL-type silver-coated nylon thread active electrode was modified to include a custom-made contact lens of optically clear Aclar film (after (Sagdullaev et al., (2004)). This was positioned concentrically on the cornea with hypromellose eye drops (1% methylcellulose solution) pre-applied. The VEP active electrode was a subcutaneous platinum needle (Grass technologies Inc.) placed in the scalp approximately 2 mm lateral to lambda, overlying a large area of the right visual cortex. Platinum needles in the scruff and at the base of the tail served as reference and ground electrodes respectively. Signals were differentially amplified and digitized at a rate of 5 kHz (VEP bandpass filtered 0–100 Hz, ERG unfiltered) using an Espion E2 system (Diagnosys LLC, Cambridge, UK). The amplitude and timing of the major ERG and VEP components was measured with the Espion software (Diagnosys LLC, Cambridge, UK) by placing a cursor at a subjectively determined turning point (i.e. the peak or trough) for each component in individual records (without knowledge of the animal's genotype). The Espion E2 system also generated and controlled the light stimulus. Brief (4 ms) single flash stimuli were delivered in a Ganzfeld dome. Animals were situated on a heated platform, maintained at a constant temperature (38 °C) using a circulating pump-water bath. All recordings were made in a custom-made, light-tight Faraday cage.

For dark-adapted testing, responses were elicited by brief flashes of white light recorded on dark background. Stimulus intensity was increased in log unit steps across a 7 log unit range (−6 to 1 log cd s/m^2, approximate scotopic units can be obtained by adding 0.44 to these values). At each intensity tested, 50 responses were averaged per result. An interstimulus interval (ISI) of 2 s was used for dimmer stimuli (−6 to −3 log cd s/m^2) and for brighter intensities (−2 to 1 log cd s/m^2) an ISI of 5 s was used. For light-adapted testing, animals were pre-exposed to steady, full-field, white background illumination (30 cd/m^2) for 10 min. Responses were then recorded to brief light flashes of three intensities (0, 1 & 1.4 log cd s/m^2) superimposed on the stable background. In all cases an ISI of 1 s was used and 50 responses were averaged per result.

2.3. In vivo imaging

Immediately after electrophysiological recordings, the fundus was imaged with a confocal scanning laser ophthalmoscope (cSLO; Spectralis-HRA, Heidelberg Engineering, Heidelberg, Germany) using a 55° angle lens. The optic disc was positioned in the centre of the image and a series of images could be obtained of various retinal layers by changing the focus. Retinal infrared (IR) reflectance images were recorded using an 810 nm laser as light source. For fundus autofluorescence (FAF) imaging a 488 nm laser was used for excitation and recording of emitted light was limited by a barrier filter to wavelengths between 500 and 700 nm. Images were recorded using the inbuilt "automatic real time" (ART) mode and enhanced using the image normalisation option, if necessary.

3. Results

3.1. Dark-adapted visual responses are normal in *Opa1*$^{+/-}$ mice

Initially, mice were exposed to brief (4 ms) flashes of white light under otherwise dark conditions. Under these dark-adapted conditions, typical ERG and flash VEP waveforms could be recorded in *Opa1*$^{+/-}$ animals. Generally, as the intensity of the light stimulus was increased there was a concomitant increase in the size and speed of ERG responses. Such intensity dependent alterations are characteristic of normal responses in wildtype animals. Comparison of representative and group averaged responses showed no clear difference between wildtype and *Opa1*$^{+/-}$ animals (Fig. 1A). Quantification of the major ERG components (a-wave and b-wave) confirmed that there was no detectable difference in the size (amplitude) or speed (implicit time) of dark-adapted ERGs across the full intensity range tested (Fig. 1B and C). Visual comparison of the amplitude and timing of oscillatory potentials (OPs) in unfiltered and 75–300 Hz bandpass filtered records indicated that these were indistinguishable between genotypes and therefore were not further analysed.

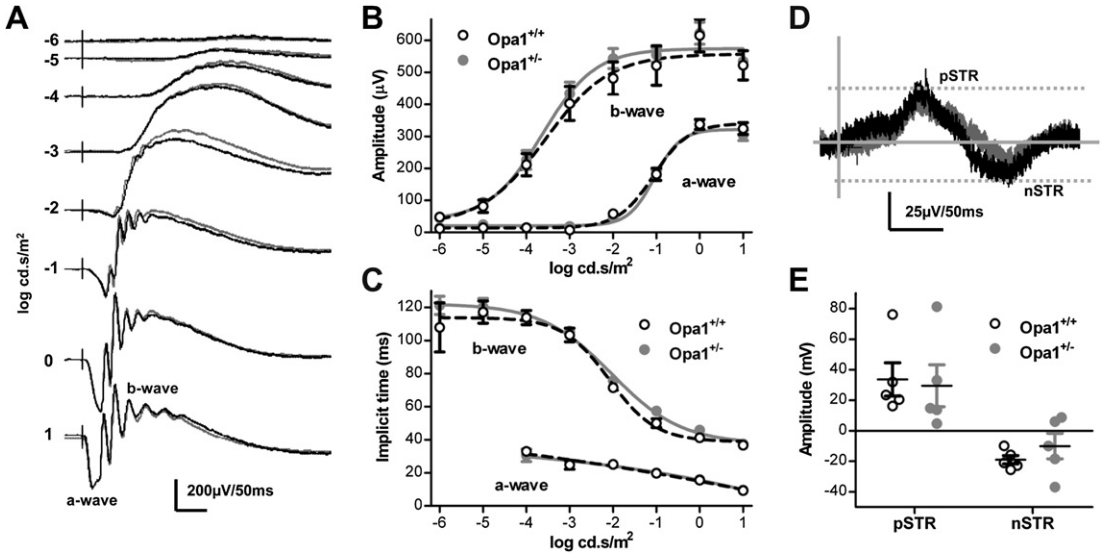

Fig. 1. Dark-adapted ERG recordings are not significantly affected in *Opa1*$^{+/-}$ mice. A. Averaged traces for each genotype ($n = 5$ for each). Stimulus intensity shown on left, values in log cd s/m^2. Quantification of B. Amplitude and C. Implicit Time of a- & b-waves. Plotted values are mean ± SEM, $n = 4$. D. Expanded view of genotype averaged ERG to dimmest stimulus (−6 log cd s/m^2) shows scotopic threshold response (STR) waveform. E. Amplitude of positive & negative STR components. Individual values plotted (n = 5), horizontal bars show group means with SEM. Wildtype control (*Opa1*$^{+/+}$) traces and values are shown in black/empty symbols, heterozygote mutants (*Opa1*$^{+/-}$) are in grey/filled symbols.

In response to very dim stimuli the dark-adapted ERG shows a very characteristic waveform known as the scotopic threshold response (STR). This waveform is thought to reflect activity of the proximal retina, i.e. amacrine and ganglion cell (Saszik et al., 2002). In response to the dimmest stimulus used (−6 log cd s/m^2) a STR could be seen in *Opa1*$^{+/-}$ and control animals (Fig. 1D). Indeed, quantification of the amplitude of the positive and negative components of the STR showed that there was no significant reduction in this waveform in heterozygous mutant mice (Fig. 1E).

Dark-adapted flash VEPs (Fig. 2A) were dominated by a strong negative component (N1) at all intensities tested. At higher intensities N1 was preceded by a small positive deflection (P1). A positive potential (P2) was also seen following the negative peak of N1. This was primarily apparent as an increasingly abrupt return to baseline (with increasing stimulus intensity) but sometimes at the highest stimuli resulted in a positive deflection above baseline. Again, as the intensity of the light stimulus was increased there was a concomitant increase in the size and speed of responses. As with the ERG, comparison of VEP responses showed no clear difference between genotypes at this age (Fig. 2A). Quantification of the size (amplitude) or speed (latency) of VEP components P1, N1 & P2 (Fig. 2B–G) confirmed that there was no significant difference between mutant and wildtype mice across the full intensity range tested.

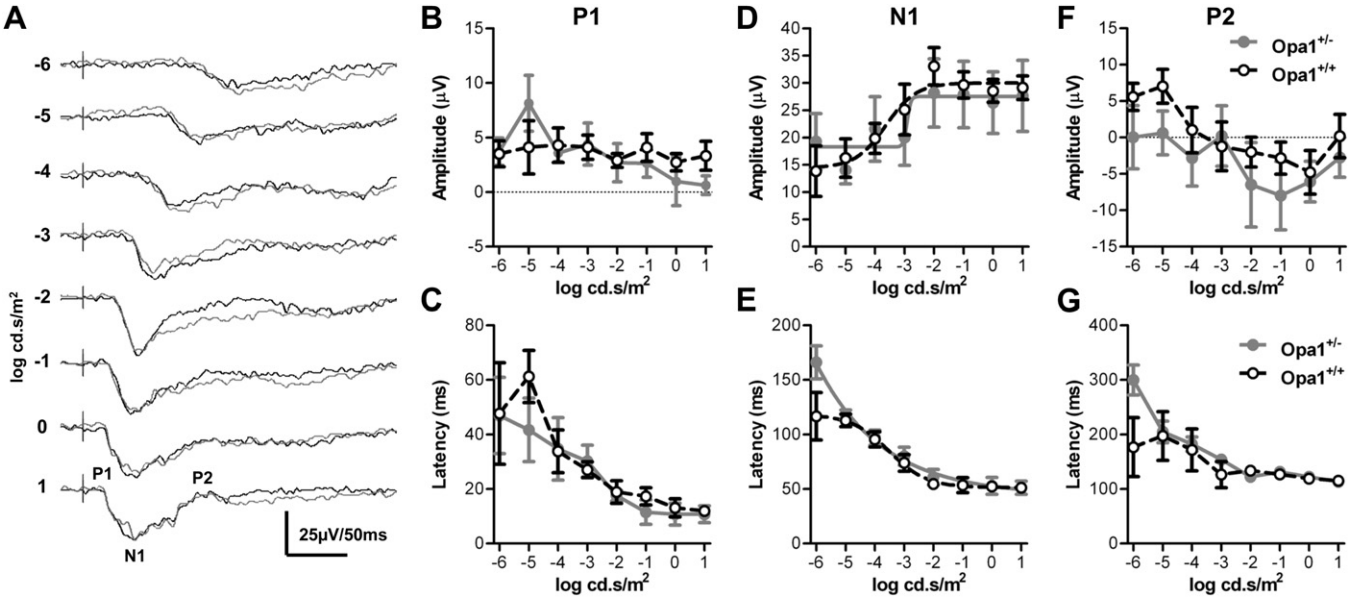

Fig. 2. Dark-adapted VEPs are not significantly affected in *Opa1*$^{+/-}$ mice. A. Averaged traces for each genotype ($n = 5$ for both). Stimulus intensity shown on left, values are log cd s/m^2. Quantification of B. Amplitude of P1. C. Latency of P1. D. Amplitude of N1. E. Latency of N1. F. Amplitude of P2. G. Latency of P2. In all graphs plotted values are mean ± SEM, $n = 5$. Wildtype control (*Opa1*$^{+/+}$) traces and values are shown in black/empty symbols, heterozygote mutants (*Opa1*$^{+/-}$) are in grey/filled symbols.

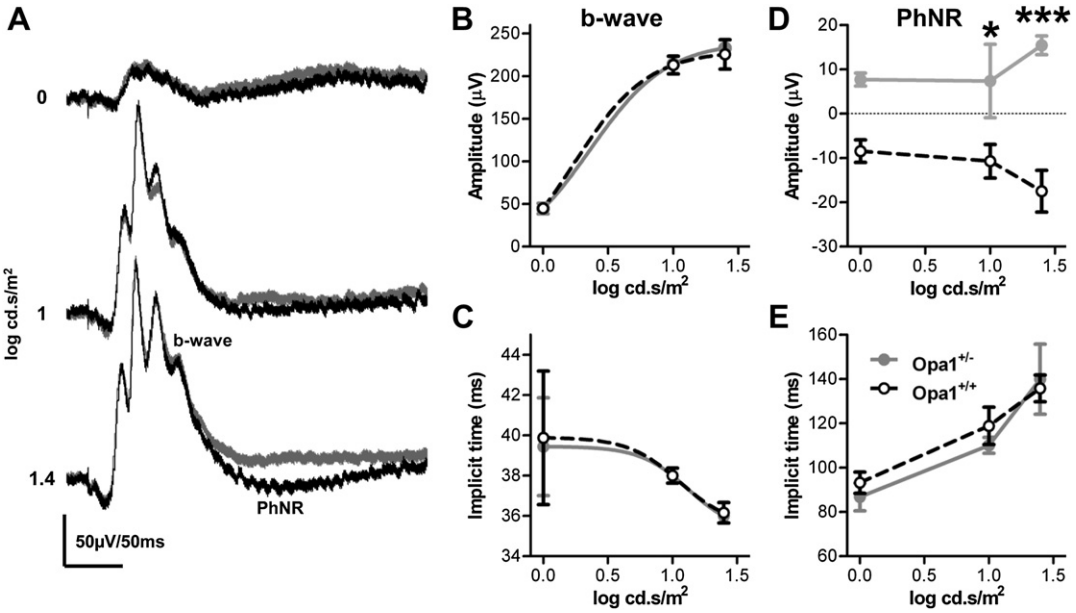

Fig. 3. *Opa1*$^{+/-}$ mice display a specific and significant reduction in the photopic negative response of the light-adapted ERG. A. Averaged traces for each genotype ($n = 5$ for both). Stimulus intensity shown on right, values are log cd s/m^2. Quantification of B. Amplitude of b-wave. C. Implicit time of b-wave. D. Amplitude of Photopic Negative Response (PhNR). E. Implicit time of PhNR. In all graphs plotted values are mean ± SEM, $n = 5$. * = $p < 0.05$, *** = $p < 0.001$: significance of Bonferroni posttests after Repeated measures Two-way ANONA with genotype and stimulus intensity as factors. Wildtype control (*Opa1*$^{+/+}$) traces and values are shown in black/empty symbols, heterozygote mutants (*Opa1*$^{+/-}$) are in grey/filled symbols.

3.2. *Opa1*$^{+/-}$ mice display specific and significant deficits in light-adapted visual responses

Following dark-adapted visual testing, mice were exposed to steady, full-field, white background illumination (30 cd/m^2). After 10 min continuous exposure, photopic visual responses were recorded to brief light flashes of different intensity, superimposed on the background. As with dark-adapted conditions, superficially normal ERG and VEP responses could be recorded from mutant animals. At all stimulus intensities, light-adapted ERGs predominantly consisted of a fast, positive b-wave with minor oscillatory potentials and little or no a-wave (Fig. 3A). Light-adapted VEPs (Fig. 4A) were similar to dark-adapted VEPs although all components were of smaller amplitude. Again, there was a clear intensity dependence of the shape, size and speed of ERG and VEP responses.

There were specific differences in the light-adapted ERG responses between heterozygous mutants and wildtype controls. Although the positive peak of the b-wave was indistinguishable between genotypes, there was a clear difference in the immediately following negative deflection – the photopic negative response (PhNR). The amplitudes and implicit times of b-waves were quantified and compared (Fig. 3B and C), which confirmed the absence of

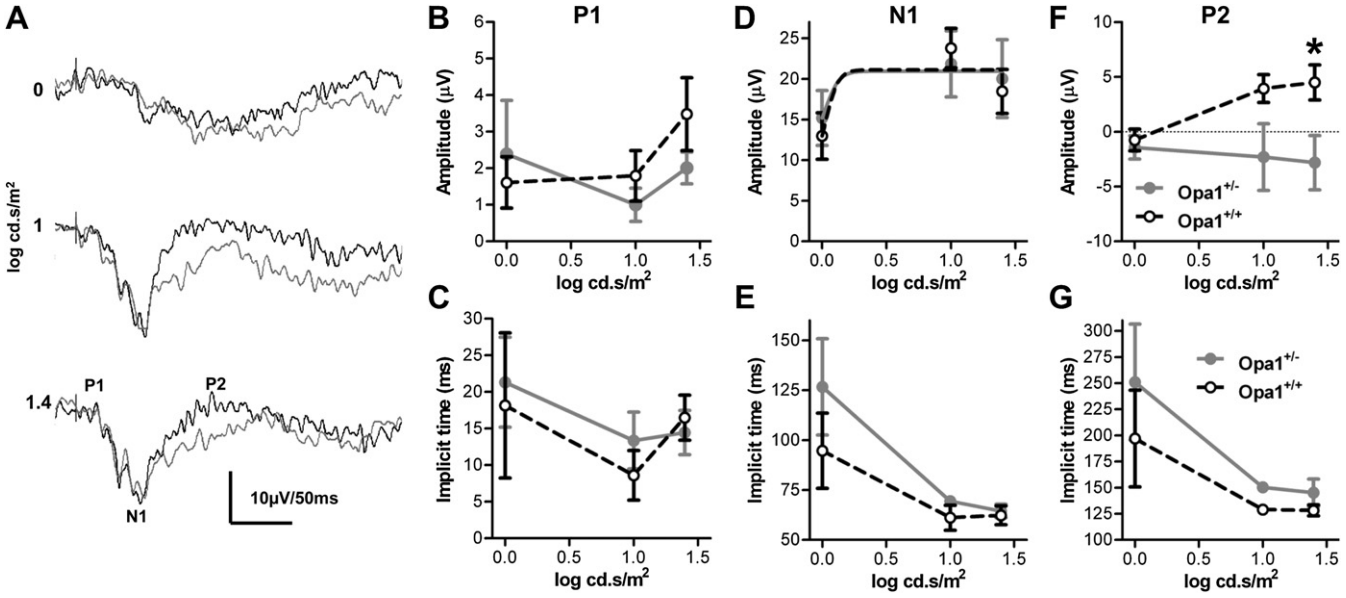

Fig. 4. *Opa1*$^{+/-}$ mice have a significant reduction in the P2 component of light-adapted VEP recordings. A. Averaged traces for each genotype ($n = 5$ for both). Stimulus intensity shown on left, values are log cd s/m^2. Quantification of B. Amplitude of P1. C. Latency of P1. D. Amplitude of N1. E. Latency of N1. F. Amplitude of P2. G. Latency of P2. In all graphs plotted values are mean ± SEM, $n = 5$. * = $p < 0.05$: significance of Bonferroni posttest after Repeated measures Two-way ANONA with genotype and stimulus intensity as factors. Wildtype control (*Opa1*$^{+/+}$) traces and values are shown in black/empty symbols, heterozygote mutants (*Opa1*$^{+/-}$) are in grey/filled symbols.

any significant difference between genotypes (Repeated measures Two-way ANOVA with genotype and stimulus intensity as factors, genotype factor $p = 0.77$, $F = 0.088$, $df = 1$ and $p = 0.90$, $F = 0.0156$, $df = 1$ for amplitude and implicit time respectively). Importantly, quantification of the PhNR amplitude (measured from baseline to negative peak) revealed a significant reduction in *Opa1*$^{+/-}$ animals relative to wildtypes at the two brightest intensities tested (Fig. 3D. Repeated measures Two-way ANOVA with genotype and stimulus intensity as factors: Interaction not significant ($p = 0.12$, $F = 2.40$, $df = 2$), stimulus intensity not significant ($p = 0.95$, $F = 0.0489$, $df = 2$), genotype highly significant ($p < 0.001$, $F = 31.3$, $df = 1$). Bonferroni posttests to compare genotypes at each stimulus intensity were as follows: 0 log cd s/m^2 not significantly different ($p > 0.05$, $t = 2.57$), 1 log cd s/m^2 significantly different ($p < 0.05$, $t = 2.88$), 1.4 log cd s/m^2 highly significantly different ($p < 0.001$, $t = 5.24$)). Quantification and comparison of the PhNR implicit times between genotypes showed that they were not different (Fig. 3E. Repeated measures Two-way ANOVA with genotype and stimulus intensity as factors, genotype factor not significant ($p = 0.60$, $F = 0.283$, $df = 2$)). Light-adapted oscillatory potentials appeared very similar between genotypes (in unfiltered and 75–300 Hz bandpass filtered records) and were not further analysed. Conversely, when we applied a 100 Hz lowpass filter to ERG records to reduce the effect of OPs, quantification of the b-wave and PhNR yielded very similar results as in unfiltered records and the statistical comparisons were equivalent to those described above (data not shown).

For light-adapted flash VEPs, another specific deficit was apparent. Although the negative N1 component appeared identical between genotypes, *Opa1*$^{+/-}$ animals showed a reduction in the subsequent positive deflection (P2 wave). Quantification of the VEP components (Fig. 4B–G) showed no significant difference in P1 and N1 amplitude or latency between *Opa1*$^{+/-}$ mice and their wildtype control at any of the stimulus intensities tested (Repeated measures Two-way ANOVA with genotype and stimulus intensity as factors, genotype factor not significant for P1 amplitude ($p = 0.50$, $F = 0.501$, $df = 1$), P1 latency ($p = 0.66$, $F = 0.212$, $df = 1$), N1 amplitude ($p = 0.89$, $F = 0.0213$, $df = 1$) or N1 latency ($p = 0.32$, $F = 1.16$, $df = 1$)). However, quantification of the P2 component (Fig. 4F and G) confirmed a significant amplitude reduction in *Opa1*$^{+/-}$ mice relative to wildtypes at the brightest intensity tested (Repeated measures Two-way ANOVA with genotype and stimulus intensity as factors: Interaction not significant ($p = 0.08$, $F = 3.08$, $df = 2$), stimulus intensity not significant ($p = 0.33$, $F = 1.19$, $df = 2$), genotype significantly different ($p < 0.05$, $F = 6.05$, $df = 1$). Bonferroni posttests to compare genotypes at each stimulus intensity were as follows: 0 log cd s/m^2 not significantly different ($p > 0.05$, $t = 0.265$), 1 log cd s/m^2 not significantly different ($p < 0.05$, $t = 2.46$), 1.4 log cd s/m^2 significantly different ($p < 0.05$, $t = 2.88$)). P2 latencies were not different between genotypes (Repeated measures Two-way ANOVA with genotype and stimulus intensity as factors, genotype factor not significant ($p = 0.29$, $F = 1.29$, $df = 2$)).

Taken together, the dark- and light-adapted recordings indicated that both rod and cone visual pathways remain largely intact and unaffected in heterozygous mutant animals at this age (one year). However, distinctive and significant differences were detected in late evolving components of the light-adapted ERG and flash VEP responses. Thus, we describe a specific and so far unreported functional visual deficit in a mouse model of ADOA.

3.3. The ocular fundi of *Opa1*$^{+/-}$ mice are indistinguishable from those of wildtype controls

Although a recent study showed no detectable retinal ganglion cell soma loss in these mice at one year (Williams et al., 2010), another study of *Opa1*$^{+/-}$ mice of a different origin identified a significant increase in retinal macrophages associated with ganglion cell loss at two years using a carbocyanine dye (Heiduschka et al., 2010). We were therefore interested to see if there was any change in macrophage distribution within the retina coincident with the above functional changes observed at one year. We used the cSLO which has recently been shown to be highly effective at identifying individual retinal macrophages *in vivo* (Luhmann et al., 2009; Xu et al., 2008). IR-reflectance images throughout the depth focus, from the retinal pigment epithelium (RPE)/outer retina to the nerve fibre layer, were comparable in mutant (Fig. 5A&B) and control animals (Fig. 5D and E). Fundus autofluorescence (FAF) imaging revealed a moderate level of background autofluorescence and the presence of a few bright foci of very high fluorescence signal. These foci were dispersed in the outer retina or distributed along retinal vessels in the inner retina/nerve fibre layer, as expected for subretinal and perivascular microglia. Although present in mutant mice, they were also found in similar locations and with similar numbers in age-matched littermate wildtype controls (Fig. 5C and F). Hence there was no evidence of low grade inflammation or signs of augmented macrophage recruitment in the retina of the *Opa1*$^{+/-}$ at this age.

4. Discussion

In this letter we describe a clear functional deficit in the PhNR of *Opa1*$^{+/-}$ mice at one year.

To our knowledge, is the first report of a phenotype detectable by ERG testing in a mouse model of ADOA. This finding is significant, because it represents an entirely retina-specific electrical response, whereas VEP recordings can be affected by mild impairment of central pathways (Lachapelle et al., 2004) where OPA1 is also widely expressed (Bette et al., 2005). Hence the PhNR may provide a useful biomarker for retinal dysfunction at early stages of dominant optic atrophy in these mice and might provide a useful measure against which to assess any retina-specific therapies, such as intravitreal gene delivery.

The precise cellular electrical generator of the PhNR has not yet been clearly identified. Although there is agreement that the potential must be derived from the proximal retina, there remains debate if it is predominantly amacrine cell or RGC in origin. There are species differences and even rodent studies have provided equivocal results; with some authors reporting a reduction in the PhNR (Li et al., 2005) while others report that it is unaffected (Mojumder et al., 2008) following optic nerve injury (to induce rapid RGC loss). Other optic nerve injury studies do not explicitly measure the PhNR (Alarcon-Martinez et al., 2010; Bui and Fortune, 2004) or are complicated by the inconsistent nature of the PhNR and the fact that it is not always reliably observed under baseline conditions, even in recording protocols that have previously been successful (Miura et al., 2009). The reasons for this are unclear, although we might speculate that factors such as time of day and long-term light history might influence the magnitude and reliability of the PhNR, as has been shown for the b-wave of the photopic ERG in mice (Barnard et al., 2006). In our study we were careful to keep these factors constant between experimental groups. These experimental precautions, combined with a prolonged recording epoch, may facilitate detection of the PhNR deficit.

Importantly, our results are phenotypically similar to the observation of a reduced PhNR in the flash ERG of patients with ADOA due to *OPA1* mutations (Miyata et al., 2007). In addition, glaucoma studies have found the PhNR to be attenuated in patients with ocular hypertension and open angle glaucoma and proposed that it can be used to quantify retinal ganglion cell dysfunction, which occurs prior to cell death in the glaucomas (Drasdo et al., 2001; North et al., 2010). Other human studies have predominantly used the pattern

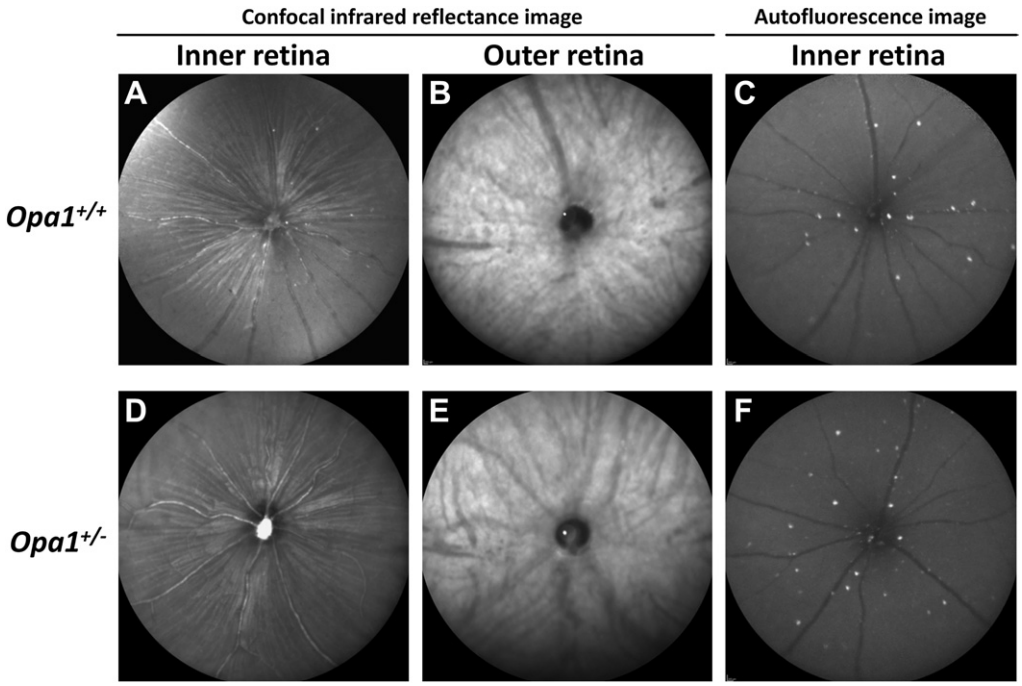

Fig. 5. The ocular fundi of *Opa1*$^{+/-}$ mice are indistinguishable from wildtype controls. Representative fundal images acquired using the cSLO. Reflectance infrared (IR) images acquired at the inner retina/nerve fibre layer confocal plane in wildtype control (A. *Opa1*$^{+/+}$) and heterozygote mutants (D. *Opa1*$^{+/-}$). Reflectance IR images acquired at the retinal pigment epithelium (RPE)/outer retina confocal plane in *Opa1*$^{+/+}$ (B.) and *Opa1*$^{+/-}$ (E.) mice. Fundus autofluorescence (FAF) images acquired at the inner retina/nerve fibre layer confocal plane in *Opa1*$^{+/+}$ (C.) and *Opa1*$^{+/-}$ (F.) mice.

electroretinogram (PERG), rather than the flash ERG used in our work. In ADOA patients the PERG shows an abnormal ratio of waveforms, with a reduction in the amplitude of the N95 waveform relative to the size of waveform P50 (Berninger et al., 1991; Holder et al., 1998; Votruba et al., 1998). As the PERG N95 component is very likely to be RGC in origin, these findings are consistent with predominantly ganglion cell death/dysfunction in ADOA. Work in non-human primates has led to the suggestion that the same cellular generators are responsible for the PhNR and the N95 of the PERG (Viswanathan et al., 2000). PERG recordings in mice are technically more demanding, the signals recorded are of very low amplitude and it is less clear how the components of the PERG relate to the flash ERG, if indeed they do (Miura et al., 2009; Porciatti, 2007). Nevertheless, PERG testing in *Opa1* mutant mice would now be useful to further explore ganglion cell function and should be attempted in future studies.

We did not observe any significant reduction in the dark-adapted scotopic threshold response (STR) in *Opa1*$^{+/-}$ mice. The STR, like the PhNR, is the subject of some discussion with regards to the most significant cellular generator (Saszik et al., 2002). Amacrine and ganglion cells are again likely contributors and the consensus of work involving pharmacology and optic nerve damage and genetic models in rodents seems to be that RGCs are relatively more important, particularly for the pSTR (Alarcon-Martinez et al., 2010, 2009; Bui and Fortune, 2004; Moshiri et al., 2008; Saszik et al., 2002). Given the proximal retinal origin, it is perhaps surprising that the STR is unaffected in *Opa1*$^{+/-}$ mice, especially given the reduction in PhNR amplitude. In fact, the observation that one amacrine/ganglion cell derived ERG component (PhNR) is affected while the other (STR) is not, is consistent with several alternative explanations. Perhaps the simplest is that the PhNR and STR are derived from separate and non-overlapping cell populations in the mouse retina that are differentially affected in heterozygous mutant mice. The observation that OPA1 is expressed in the ganglion cell layer (GCL), inner plexiform layer (IPL), and inner nuclear layer (INL) of the retina (Aijaz et al., 2004) may be relevant to this. Alternatively, at this age mutant mice may display a STR deficit which is too subtle to be detected in our recordings; stimulus paradigms that focus specifically on the range of stimuli eliciting n and pSTRs might show the differences more readily. It would be of great interest but, to our knowledge, the STR of the flash ERG has not yet been studied in ADOA patients.

Our principal finding in VEP recordings was that function is predominantly unaltered in *Opa1*$^{+/-}$ mice. N1, the main component of the mouse flash VEP, was not significantly different from controls, in terms of both amplitude and latency, under all conditions tested. In patients with ADOA, the amplitude and/or latency of multiple components of the VEP can be affected (Granse et al., 2003; Holder et al., 1998; Votruba et al., 1998). Differences in the stimuli used (flash vs. pattern) and large species differences in the resultant VEP waveforms belie a detailed comparison with our results. However, we did detect a defined VEP phenotype (significant reduction in the-amplitude of P2 in *Opa1*$^{+/-}$ mice relative to wildtype controls), further confirming the face validity of our mouse line as a model of ADOA. Although this deficit is subtle, it could foreshadow a more generalised impairment of the VEP, with increasing age/disease progression.

Heiduschka et al. (2010) reported a 50% reduction in the P1-N1 amplitudes of dark-adapted VEPs in *Opa1* mutant mice at higher light intensities and a statistically insignificant trend towards smaller amplitudes in light-adapted VEPs. They note that the P2 amplitudes showed no difference, but the quantitative data were not shown. VEP latency was not affected in mutant mice in their study, which is in agreement with our results. Mice used in their study were substantially older (>20 months old) than those used here (11–13 months old) which perhaps accounts for the difference in terms of P1-N1/N1 amplitude findings. However, the fact that they do not detect a significant reduction in P2 amplitude cannot be explained by age differences, but is perhaps due to differences in

the precise mouse model used or because of minor technical differences between the studies.

Taken together with normal ERG findings, Heiduschka et al. (2010) say that their VEP data indicate the number of RGCs that transmit the signal has to be reduced and also implies that the remaining RGCs function normally. This is applicable in the context of significant RGC loss but does not explain functional deficits when no death of RGC can be detected. This is important, as previous work shows that no significant loss of ganglion cells can be detected in the ADOA model used, at the age we tested or even older (White et al., 2009; Williams et al., 2010). Therefore, our preferred interpretation of the functional deficits we observe is that they are due to altered function in RGCs, rather than RGC death. Altered RGC function may be related to pathophysiology in cellular processes associated with defects in mitochondrial fusion. A morphological basis for altered RGC function is also provided by the recent finding of dendropathy and increased dendritic pruning specifically in ON-centre RGCs in the *Opa1*$^{+/-}$ mouse (Williams et al., 2010).

5. Conclusions

To our knowledge this is the first report of a functional deficit detectable with the ERG in a mouse model of ADOA. The reduction in PhNR amplitude is indicative of ganglion cell dysfunction and is similar to the phenotype observed in some ADOA patients (Miyata et al., 2007). The deficit is apparent in *Opa1*$^{+/-}$ mice at one year, which coincides with an increase in dendritic retraction/pruning in retinal ganglion cells, which has been previously reported to occur at a similar age in the same mutant mouse line (Williams et al., 2010). A functional phenotype that is detectable by ERG offers particular benefits as it is less invasive than cortical electrode VEP recording. Importantly, with ERG, treatments of one eye can be compared with the untreated partner eye in the same animal. Thus, the ERG phenotype we have described may be useful in the robust and accurate assessment of potential treatments for ADOA.

Acknowledgements

We would like to thank the following sources of funding: The Royal College of Surgeons of Edinburgh, the Health Foundation, the NIHR Biomedical Research Centres, Marie Curie Intra-European Fellowship (no.: 237238); the Seventh European Community Framework Program; European Commission, Fight for Sight, Medical Research Council UK (Grant no.: G0700949), the Biotechnology and Biological Sciences Research Council (Grant no.: BB/G003602/1) and the Wellcome Trust (Grant no.: 091984/Z/10/Z).

References

Aijaz, S., Erskine, L., Jeffery, G., Bhattacharya, S.S., Votruba, M., 2004. Developmental expression profile of the optic atrophy gene product: OPA1 is not localized exclusively in the mammalian retinal ganglion cell layer. Invest. Ophthalmol. Vis. Sci. 45, 1667–1673.

Alarcon-Martinez, L., Aviles-Trigueros, M., Galindo-Romero, C., Valiente-Soriano, J., Agudo-Barriuso, M., Villa Pde, L., Villegas-Perez, M.P., Vidal-Sanz, M., 2010. ERG changes in albino and pigmented mice after optic nerve transection. Vision Res. 50, 2176–2187.

Alarcon-Martinez, L., de la Villa, P., Aviles-Trigueros, M., Blanco, R., Villegas-Perez, M.P., Vidal-Sanz, M., 2009. Short and long term axotomy-induced ERG changes in albino and pigmented rats. Mol. Vis. 15, 2373–2383.

Alexander, C., Votruba, M., Pesch, U.E., Thiselton, D.L., Mayer, S., Moore, A., Rodriguez, M., Kellner, U., Leo-Kottler, B., Auburger, G., Bhattacharya, S.S., Wissinger, B., 2000. OPA1, encoding a dynamin-related GTPase, is mutated in autosomal dominant optic atrophy linked to chromosome 3q28. Nat. Genet. 26, 211–215.

Amati-Bonneau, P., Milea, D., Bonneau, D., Chevrollier, A., Ferre, M., Guillet, V., Gueguen, N., Loiseau, D., de Crescenzo, M.A., Verny, C., Procaccio, V., Lenaers, G., Reynier, P., 2009. OPA1-associated disorders: phenotypes and pathophysiology. Int. J. Biochem. Cell Biol. 41, 1855–1865.

Barnard, A.R., Hattar, S., Hankins, M.W., Lucas, R.J., 2006. Melanopsin regulates visual processing in the mouse retina. Curr. Biol. 16, 389–395.

Berninger, T.A., Jaeger, W., Krastel, H., 1991. Electrophysiology and colour perimetry in dominant infantile optic atrophy. Br. J. Ophthalmol. 75, 49–52.

Bette, S., Schlaszus, H., Wissinger, B., Meyermann, R., Mittelbronn, M., 2005. OPA1, associated with autosomal dominant optic atrophy, is widely expressed in the human brain. Acta Neuropathol. 109, 393–399.

Bui, B.V., Fortune, B., 2004. Ganglion cell contributions to the rat full-field electroretinogram. J. Physiol. 555, 153–173.

Davies, V., Votruba, M., 2006. Focus on molecules: the OPA1 protein. Exp. Eye Res. 83, 1003–1004.

Davies, V.J., Hollins, A.J., Piechota, M.J., Yip, W., Davies, J.R., White, K.E., Nicols, P.P., Boulton, M.E., Votruba, M., 2007. Opa1 deficiency in a mouse model of autosomal dominant optic atrophy impairs mitochondrial morphology, optic nerve structure and visual function. Hum. Mol. Genet. 16, 1307–1318.

Drasdo, N., Aldebasi, Y.H., Chiti, Z., Mortlock, K.E., Morgan, J.E., North, R.V., 2001. The s-cone PHNR and pattern ERG in primary open angle glaucoma. Invest. Ophthalmol. Vis. Sci. 42, 1266–1272.

Granse, L., Bergstrand, I., Thiselton, D., Ponjavic, V., Heijl, A., Votruba, M., Andreasson, S., 2003. Electrophysiology and ocular blood flow in a family with dominant optic nerve atrophy and a mutation in the OPA1 gene. Ophthalmic Genet. 24, 233–245.

Heiduschka, P., Schnichels, S., Fuhrmann, N., Hofmeister, S., Schraermeyer, U., Wissinger, B., Alavi, M.V., 2010. Electrophysiological and histologic assessment of retinal ganglion cell fate in a mouse model for OPA1-associated autosomal dominant optic atrophy. Invest. Ophthalmol. Vis. Sci. 51, 1424–1431.

Holder, G.E., Votruba, M., Carter, A.C., Bhattacharya, S.S., Fitzke, F.W., Moore, A.T., 1998. Electrophysiological findings in dominant optic atrophy (DOA) linking to the OPA1 locus on chromosome 3q 28-qter. Doc. Ophthalmol. 95, 217–228.

Lachapelle, J., Ouimet, C., Bach, M., Ptito, A., McKerral, M., 2004. Texture segregation in traumatic brain injury – a VEP study. Vision Res. 44, 2835–2842.

Li, B., Barnes, G.E., Holt, W.F., 2005. The decline of the photopic negative response (PhNR) in the rat after optic nerve transection. Doc. Ophthalmol. 111, 23–31.

Luhmann, U.F., Robbie, S., Munro, P.M., Barker, S.E., Duran, Y., Luong, V., Fitzke, F.W., Bainbridge, J.W., Ali, R.R., MacLaren, R.E., 2009. The drusenlike phenotype in aging Ccl2-knockout mice is caused by an accelerated accumulation of swollen autofluorescent subretinal macrophages. Invest. Ophthalmol. Vis. Sci. 50, 5934–5943.

Miura, G., Wang, M.H., Ivers, K.M., Frishman, L.J., 2009. Retinal pathway origins of the pattern ERG of the mouse. Exp. Eye Res. 89, 49–62.

Miyata, K., Nakamura, M., Kondo, M., Lin, J., Ueno, S., Miyake, Y., Terasaki, H., 2007. Reduction of oscillatory potentials and photopic negative response in patients with autosomal dominant optic atrophy with OPA1 mutations. Invest. Ophthalmol. Vis. Sci. 48, 820–824.

Mojumder, D.K., Sherry, D.M., Frishman, L.J., 2008. Contribution of voltage-gated sodium channels to the b-wave of the mammalian flash electroretinogram. J. Physiol. 586, 2551–2580.

Moshiri, A., Gonzalez, E., Tagawa, K., Maeda, H., Wang, M., Frishman, L.J., Wang, S.W., 2008. Near complete loss of retinal ganglion cells in the math5/brn3b double knockout elicits severe reductions of other cell types during retinal development. Dev. Biol. 316, 214–227.

North, R.V., Jones, A.L., Drasdo, N., Wild, J.M., Morgan, J.E., 2010. Electrophysiological evidence of early functional damage in glaucoma and ocular hypertension. Invest. Ophthalmol. Vis. Sci. 51, 1216–1222.

Porciatti, V., 2007. The mouse pattern electroretinogram. Doc. Ophthalmol. 115, 145–153.

Sagdullaev, B.T., DeMarco, P.J., McCall, M.A., 2004. Improved contact lens electrode for corneal ERG recordings in mice. Doc. Ophthalmol. 108, 181–184.

Saszik, S.M., Robson, J.G., Frishman, L.J., 2002. The scotopic threshold response of the dark-adapted electroretinogram of the mouse. J. Physiol. 543, 899–916.

Viswanathan, S., Frishman, L.J., Robson, J.G., 2000. The uniform field and pattern ERG in macaques with experimental glaucoma: removal of spiking activity. Invest. Ophthalmol. Vis. Sci. 41, 2797–2810.

Votruba, M., 2004. Molecular genetic basis of primary inherited optic neuropathies. Eye (Lond) 18, 1126–1132.

Votruba, M., Fitzke, F.W., Holder, G.E., Carter, A., Bhattacharya, S.S., Moore, A.T., 1998. Clinical features in affected individuals from 21 pedigrees with dominant optic atrophy. Arch. Ophthalmol. 116, 351–358.

White, K.E., Davies, V.J., Hogan, V.E., Piechota, M.J., Nichols, P.P., Turnbull, D.M., Votruba, M., 2009. OPA1 deficiency associated with increased autophagy in retinal ganglion cells in a murine model of dominant optic atrophy. Invest. Ophthalmol. Vis. Sci. 50, 2567–2571.

Williams, P.A., Morgan, J.E., Votruba, M., 2010. Opa1 deficiency in a mouse model of dominant optic atrophy leads to retinal ganglion cell dendropathy. Brain 133, 2942–2951.

Xu, H., Chen, M., Manivannan, A., Lois, N., Forrester, J.V., 2008. Age-dependent accumulation of lipofuscin in perivascular and subretinal microglia in experimental mice. Aging Cell 7, 58–68.

Yin, L., Greenberg, K., Hunter, J.J., Dalkara, D., Kolstad, K.D., Masella, B.D., Wolfe, R., Visel, M., Stone, D., Libby, R.T., Diloreto Jr., D., Schaffer, D., Flannery, J., Williams, D.R., Merigan, W.H., 2011. Intravitreal injection of AAV2 transduces macaque inner retina. Invest. Ophthalmol. Vis. Sci.

Yu-Wai-Man, P., Griffiths, P.G., Gorman, G.S., Lourenco, C.M., Wright, A.F., Auer-Grumbach, M., Toscano, A., Musumeci, O., Valentino, M.L., Caporali, L., Lamperti, C., Tallaksen, C.M., Duffey, P., Miller, J., Whittaker, R.G., Baker, M.R., Jackson, M.J., Clarke, M.P., Dhillon, B., Czermin, B., Stewart, J.D., Hudson, G., Reynier, P., Bonneau, D., Marques Jr., W., Lenaers, G., McFarland, R., Taylor, R.W., Turnbull, D.M., Votruba, M., Zeviani, M., Carelli, V., Bindoff, L.A., Horvath, R., Amati-Bonneau, P., Chinnery, P.F., 2010. Multi-system neurological disease is common in patients with OPA1 mutations. Brain 133, 771–786.